

Synthesis and characterization of ZnO nanoparticles for Optical application by using Sol-gel Process

^{1*} F. Celin Hemalatha & ² Dr. A. J. Clement Lourduraj

^{1,2} Assistant Professor, PG & Research Department of Physics, St. Joseph's College (Autonomous),
Affiliated to the Bharathidasan University, Tiruchirappalli – 2

Corresponding author E.mail: celinhema@gmail.com

ABSTRACT

Zinc oxide plays an important role in current industry due to its special characteristics. Therefore, the objective of this study is to synthesize zinc oxide nanostructures with the most practical ways by using sol-gel method and characterize the nanostructures. ZnO nanoparticles were synthesized via sol-gel method using Zinc acetate dehydrate ($Zn(CH_3COO)_2 \cdot 2H_2O$) as a precursor and ethanol (CH_2COOH) was used as a solvent, Sodium hydroxide (NaOH) and distilled water were used as a medium. ZnO nanoparticles were characterized by using UV, FTIR and XRD result spectrum displays mainly oxygen and zinc peaks, which indicate the crystallinity in nature as exhibited. The XRD data shown that the average size of the nanoparticles is 25.25nm. The obtained ZnO nanoparticles are homogenous and consistent in size which corresponds to the XRD result that exhibits good crystallinity.

Keywords: Sol-gel, ZnO NPs, XRD, FTIR, UV, Band gap energy etc.,

1. INTRODUCTION

High demands of nanomaterials have produced enormous applications in global industries. Due to high demand as NPs based products, various types of engineered nanoparticles (ENPs) are synthesized for myriad of applications [1]. These days, ZnO NPs have become a promising candidate and gained more attention especially in nanomedicine and nano-semiconductors [2–4]. ZnO NPs exhibit wurtzite crystal structure that has been widely used in industries due to its unique optoelectric properties [5]. ZnO NPs are among of various semiconductivity materials with a distinctive electronic and photonic wurtzite semiconductor with a wide direct band gap (3.37eV) and high exciton binding energy (60 meV) at room temperature [6]. This makes ZnO NPs particularly popular for use in commercially available especially in sunscreens and cosmetics which able to block UV radiation when they are less than 50 nm [7–9]. Heiligttag et al [10] stated that smaller size of NPs provide a better protection of skin against UV damage.

Besides, high optical absorption UVA and UVB in ZnO NPs are also beneficial in antimicrobial products in nanomedicine as nowadays various nanomaterials development have been applied to improve drugs and other medicine [11] Among other MO NPs, Salem et al.[12] stated that ZnO NPs are the most recommended for antibacterial agent. Hence, the increase productions of consumer products eventually increase the productions of ZnO NPs. Heiligttag et al.10 has also stated

that the potential applications of ZnO NPs make them one of a primary focus in NPs research. Naveed Ul Haqet al.[13] also described that ZnO NPs is one of the cheap materials that this causes the extensive productions in industries. Morphologically, ZnO NPs is an attractive compound that possess thermal and chemical stability [14]. ZnO NPs are made into various shapes and sizes depending on the use of NPs in industries including textile, energy, food, cosmetics, and medicines and other characteristics that make them attractive for broad range of application [15].

Various synthesis methods of ZnO NPs were developed into different size and forms in order to be used in commercial products. This includes sol-gel method, precipitation, microwave assisted, and thermal oxidation.⁴ However, these methods are considered complicated as they involve multiple steps procedures, lengthy reaction period, and toxic solvent and reactants might be used for synthesis [16,17]. Prominent methods usually have undergone approximately 24 hours of reaction time, The aim of this research is to synthesize spherical ZnO NPs with less than 10 nm size by using zinc acetate dihydrate and Sodium hydroxide with a absolute ethanol as solvent via solvothermal method and to characterize synthesized ZnO NPs using few techniques including XRD, FT-IR, and UV-Vis spectroscopy, etc.,

2. MATERIALS AND METHODS

Nanostructure ZnO nanoparticles can be synthesized by using many methods such as hydrothermal, sol-gel, solvothermal. Among all methods, I have chosen sol-gel method. It offers several advantages like better homogeneity, high purity, phase pure powder at low temperatures, controlled stoichiometry. It is the simplest method, consume less power and can be carried out in robust atmosphere. It has the ability to control the particle size and morphological through systematic monitoring of reaction parameters.

2.1 Materials Required

Zinc Acetate Dihydrate ($\text{Zn}(\text{CH}_3\text{COO})_2 \cdot 2\text{H}_2\text{O}$), Sodium Hydroxide (NaOH), pH meter, distilled water are all analytical grades and used for synthesis without further purification.

2.1.1 Synthesis of pure ZnO nanoparticles

Zinc oxide nanostructure was synthesized by using sol-gel method. In order to prepare a sol, 4.23 grams of Zinc acetate dihydrate was dissolved in 100ml of distilled water by constant stirred for half an hour. 4 grams of NaOH pellets were dissolved in 100ml of distilled water by vigorous stirred for 15 minutes. This solution was added drop by drop to above prepared solution to achieve the pH nearly 12. The pH test was carried out with the help of pH tester. The solution was further stirred

for one hour and the precipitate was obtained. The entire process was carried out only at room temperature and ambient conditions. Collected precipitate was washed many times by distilled water and centrifuged. This was repeated for two or more times. After that the white solid product was collected and dried in hot air oven at 120°C. The fine powder was made by grinding the dried precipitate and was used for further characterization.

2.2 UV Visible spectroscopy analysis

UV-visible spectra of sample were monitored as a function of time of reaction on the UV-visible spectroscopy and the investigation was carried out using PERKIN ELMER (Lambda 35 model) spectrometer in the range of 190 nm to 1100 nm.

2.3 FT-IR Measurement

The Fourier transform infrared (FTIR) investigation is carried out using PERKIN ELMER (Spectrum RXI) spectrometer in the range of 400 cm⁻¹ to 4000 cm⁻¹. The functional groups were identified using the peak assignments

2.4 XRD Measurement

The sample was drop- coated onto Nickel plate by just dropping a small amount of sample on the plate frequently, allowed to dry and finally thick coat of sample was prepared. The particle size and nature of the silver nanoparticle was determined using Xray diffraction (XRD). This was carried out using Rigaku miniflex-3 model with 30kv, 30mA with Cuk α radians at 2 θ angle.

3. RESULT AND DISCUSSION

3.1 UV-visible Spectroscopy analysis

The wavelength of UV is shorter than the visible light. It ranges from 100 to 400 nm. In a standard UV-V is spectrophotometer, a beam of light is split; one half of the beam (the sample beam) is directed through a transparent cell containing a solution of the compound being analysed, and one half (the reference beam) is directed through an identical cell that does not contain the compound but contains the solvent. The instrument is designed so that it can make a comparison of the intensities of the two beams as it scans over the desired region of the wavelengths. If the compound absorbs light at a particular wavelength, the intensity of the sample beam (IS) will be less than that of the reference beam [18]. Absorption of radiation by a sample is measured at various wavelengths and plotted by a recorder to give the spectrum which is a plot of the wavelength of the entire region versus the absorption (A) of light at each wavelength. And the band gap of the sample can be obtained by plotting the graph between ($\alpha h\nu$ vs $h\nu$) and extrapolating it along x-axis. Ultraviolet and visible spectrometry is almost entirely used for quantitative analysis; that is, the estimation of the amount of a compound known to be present in the sample. The sample is usually examined in solution.

3.1.1 UV-visible characterization pure ZnO nanoparticle

The UV-visible transmission and absorption of ZnO nanopowder is presented below. The sample absorbs the radiations in the UV range upto 365.65 nm and almost all the visible spectrum radiations are transmitted by the ZnO nanoparticles.

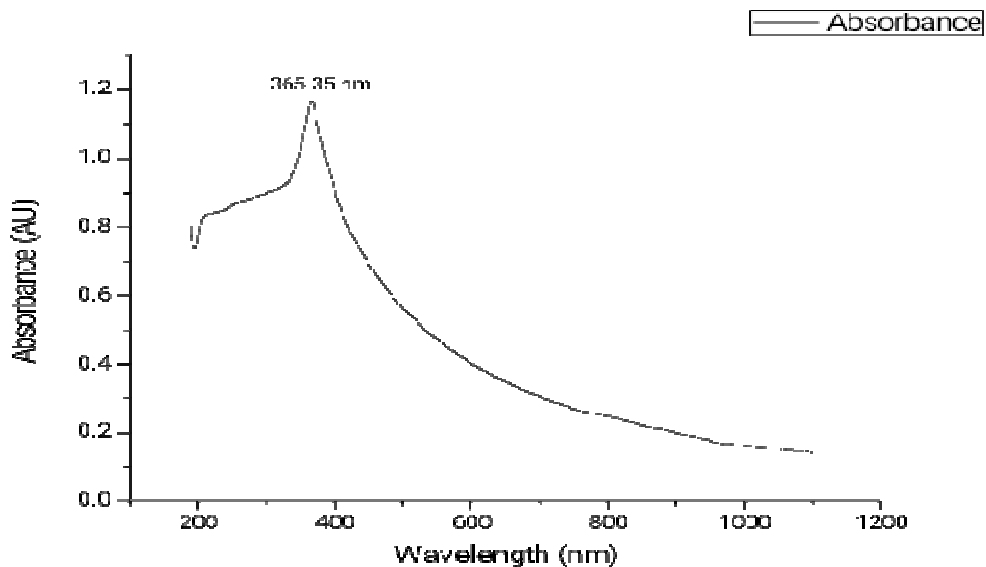


Fig: 1 Absorbance of UV-visible spectra of pure ZnO nanoparticle (Absorbance vs Wavelength Graph)

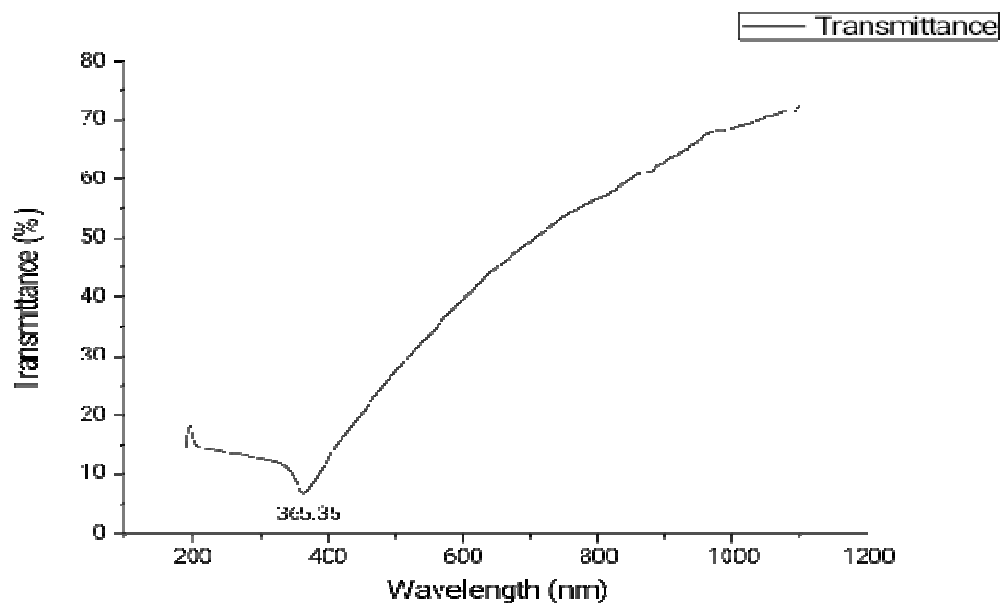


Fig: 2 Transmittance of UV-visible spectra of pure ZnO nanoparticle (Absorbance vs Wavelength Graph)

3.2 Bandgap energy:

UV-visible spectroscopy analysis has done for pure ZnO nanoparticles and the absorption peaks has found at 365.35 nm for pure ZnO nanoparticle.

Optical bandgap has been calculated with bandgap calculation formula,

hc

$$E = \frac{hc}{\lambda}$$

Where,

E is energy

h is planck's constant = 6.626×10^{-34} Joules sec

c is velocity of light = 2.99×10^8 m/s

λ is wavelength = Absorption value, $1\text{eV} = 1.6 \times 10^{-19}$ Joules

Using Tauc plots bandgap can be calculated via UV-visible spectroscopy by plotting graph. Thus Pb doped ZnO nanoparticle the energy bandgap is well optimized and increase in bandgap can be found.

By drawing graph between Energy vs $(\alpha h\nu)^2$ and taking the tangent we found the energy bandgap of nanoparticles. In similar way pure ZnO and Pb doped ZnO nanoparticle bandgap has been found.

The band gap is found to be 3.39 eV absorption peak at 365.56nm for Pure ZnO for the samples calcined at 700°C and 900°C for 4 hrs respectively. Thereby indicates that band gap remains almost same with increasing annealing temperature. Thus, from the value of band gap obtained 3.17eV agrees with the earlier reports [19] of the material.

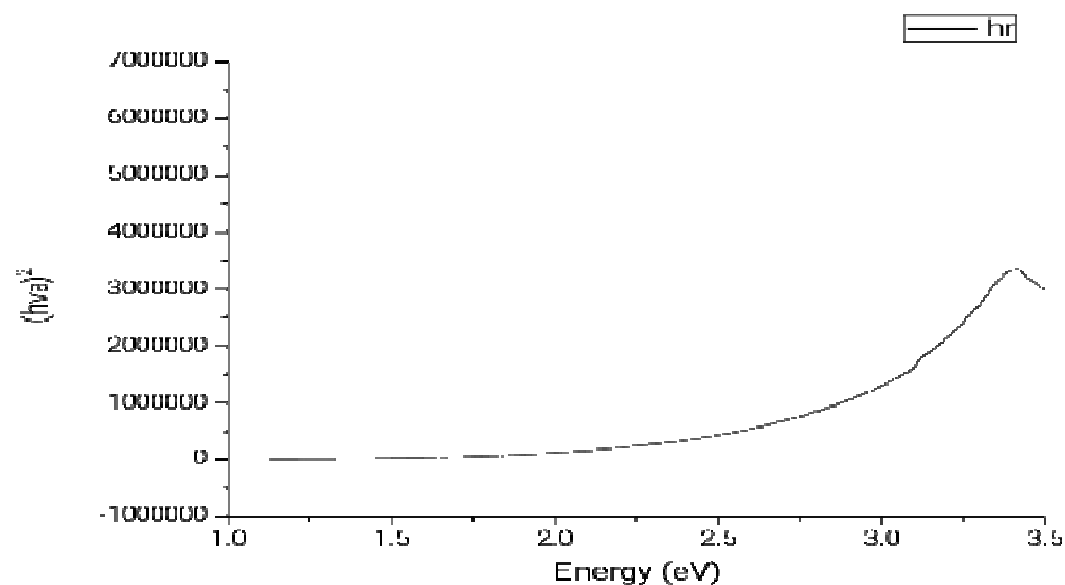


Fig: 5 Absorption of UV-visible spectra of pure ZnO for Band cap energy

3.3 FTIR characterization

3.3.1 Pure ZnO nanoparticles:

In the region of longer wavelength or low frequency the identification of different types of chemicals is possible by this technique of infrared spectroscopy and the instrument requires for its execution is Fourier transform infrared (FTIR) spectrometer. The spectroscopy merely based on the fact that molecules absorb specific frequencies that are characteristic of their structure termed as resonant frequencies, i.e. the frequency of the absorbed radiation matches the frequency of the bond or group that vibrates. And the detection of energy is done on the basis of shape of the molecular potential energy surfaces, the masses of the atoms, and the associated vibronic coupling.

Fourier transform infrared (FTIR) spectroscopy was performed to study the prepared ZnO nanoparticles and the corresponding spectra are shown in figure 7.8. The broad envelope in the higher energy region about 3500 cm^{-1} due to O-H group which represents the presence of water molecules on the surface of ZnO nanoparticles. Strong bands from 1500 cm^{-1} to 1700 cm^{-1} which corresponds to the functional group of C-O symmetric and antisymmetric stretching mode. Presence of water is also evident by its sharp peak about 1623 cm^{-1} . The secondary vibrations of Zn-O bond are found to be lying at $541,07\text{ cm}^{-1}$ and indicates the product is well crystallized. Hence the water might control the size of ZnO during the synthesis.

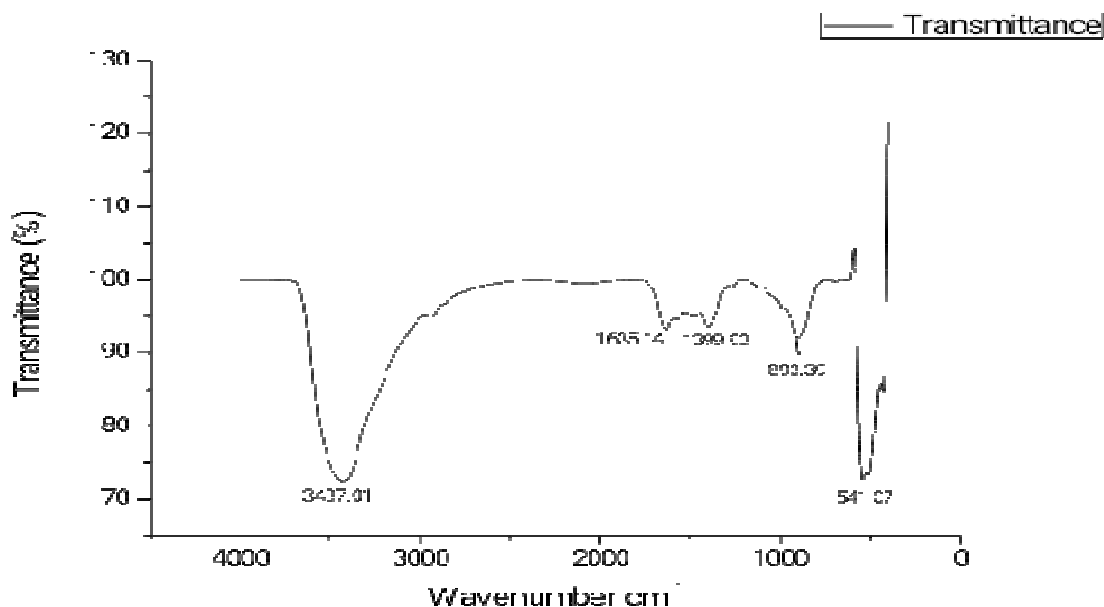
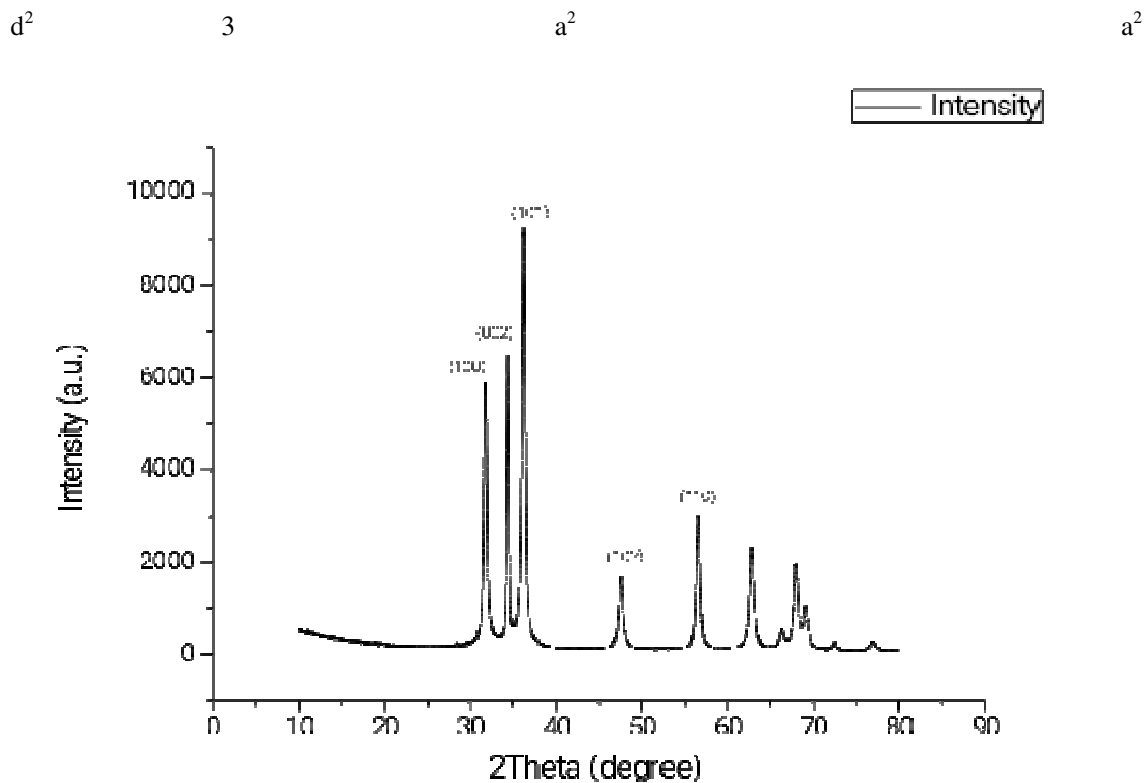


Fig:7 Enlargement of FTIR spectra of the prepared pure ZnO nanoparticles

3.4 XRD characterization:

Structural parameters such as lattice parameters and unit cell volumes for hexagonal ZnO nanoparticles are calculated from the lattice geometry equations.

$$\frac{1}{d^2} = \frac{4}{a^2} \left[\frac{h^2+hk+k^2}{3} \right] + \frac{c^2}{4d^2}$$



where a and c are the lattice parameters. h, k and l are the miller indices and d_{hkl} is the interplanar spacing.

The Debye Scherrer's formula was used to calculate the crystalline size (D) from full width half maxima (FWHM) of major XRD peak.

$$D = \frac{K\lambda}{\beta \cos\theta}$$

Where D = crystalline size

λ = X-ray wavelength

β = Full Width Half Maxima

θ = Bragg diffraction angle

K = shape factor whose value is 0.9

Hence from the above study shows that the ZnO and Pb doped ZnO helps in controlling the size of nanoparticles.

3.4.1 XRD characterization of pure ZnO

The structural composition of the samples was confirmed from XRD studies. The XRD pattern of ZnO nanoparticles synthesized which shows peaks at 31.7339° , 34.3741° , 36.2232° , 47.4903° , 56.5502° which corresponds to (100), (002), (101), (102) and (101) plane respectively. So, the X-ray diffraction of synthesized ZnO nanoparticles Hexagonal wurtzite structure according to JCPDF data (card number PDF#800075ICDS#067849). The unit cell parameters are $a=b=0.3253$ nm and $c=0.5209$ nm. The full width at half maximum was measured using Gaussian curve for the highest

peak 101. The observed peak position are in good agreement with the hexagonal wurtzite structure. The average size of nanoparticles was found to be equal to 25.25 nm.

The average crystallite size increases with increase in calcination temperature. A significant increase in crystallite size is observed for the sample calcined at 900°C. At such high temperatures, migration of grain boundaries occurs, causing the coalescence of small grains and formation of large grains.

Fig: 9 XRD pattern of pure ZnO

4. Conclusions

Zinc oxide nanoparticles were synthesized through sol-gel method by considering different calcinations temperatures. The absorption measurements were carried out using UV-Visible spectrophotometer to check the stability of nanoparticles. Characteristic UV-Vis spectrum peak of ZnO nanoparticles at 365.35nm, due to the inter-band $4d \rightarrow 5sp$ transitions; and the red shift in this peak to around 365 nm was observed due to the occurring of the plasmonic resonance phenomenon in the nano-dispersion of metal. From FTIR, the secondary vibrations of Zn-O bond are found to be lying at $541,07 \text{ cm}^{-1}$ and indicates the product is well crystallized. This sharp bands positioned at 436 cm^{-1} is associated with the characteristic wurtzite lattice vibrations ZnO. The results of the XRD showed that the average particle size of ZnO particles is 25.25 nm and also size increases with increasing calcinations temperature, and Furthermore, the FTIR showed a broad absorption band related to Zn-O vibration band. The band gap of the zinc oxide nanoparticles was estimated from the UV-VIS absorption. It was observed that the band gap of the samples remains almost constant i.e (3.39eV) for different calcination temperature from 700°C to 900°C.

5. REFERENCES

1. M. A. Maurer-Jones, I. L. Gunsolus, C. J. Murphy, C. L. Haynes, *Anal. Chem.*, 2013, 85, 3036–3049.
2. B. Liu & H. C. Zeng, *J. Am. Chem. Soc.*, 2003 125, 4430–4431.
3. V. Sharma, R. K. Shukla, N. Saxena, *Toxicol. Lett.*, 2009, 185, 211–218.
4. S. Talam, S. R. Karumuri, & N. Gunnam, *ISRN Nano*, 2012, 1–6.
5. H. Ma, P. L. Williams, S. A. Diamond. *Environ. Pollut.*, 2013, 172, 76–85.
6. A. Kołodziejczak-Radzimska, T. Jesionowski, *Mater*, 2014, 7, 2833–2881.
7. L. K. Adams, D. Y. Lyon, P. J. Alvarez, *Water Res.*, 2006, 40, 3527–3532.
8. I. Blinova, A. Ivask, M. Heinlaan, M. Mortimer, A. Kahru, *Environ. Pollut.*, 2010, 158, 41–47.
9. L. C. Wehmas, C. Anders, J. Chess, A. Punnoose, C. B. Pereira, J. A. Greenwood, R. L. Tanguay, *Toxicol Rep*, 2015, 2, 702– 715.
10. F. J. Heiligtag & M. Niederberger, *Mater. Today*, 2013, 16, 262–271.

11. S. Gunalan, R. Sivaraj, V. Rajendran, *Mater Int.*, 2012, 22, 693–700.
12. W. Salem, D. R. Leitner, F. G. Zingl, G. Schratte, R. Prassl, W. Goessler, S. Schild, *Int J Med Microbiol*, 2015, 305, 85–95.
13. A. Naveed Ul Haq, A. Nadhman, I. Ullah, G. Mustafa, M. Yasinzai, & I. Khan. J. *Nanomater.*, 2017.
14. A. Šarić, G. Štefanić, G. Dražić, & M. Gotić, *J. Alloys Compd*, 2015, 652, 91–99.
15. E. Hughes, Big problems with little particles? *Chemistry World*, <http://www.rsc.org/chemistryworld/2015/04/nanoparticle-toxicology> (assessed: September 16, 2017)
16. K. D. Bhatte, D. N. Sawant, R. A. Watile, B. M. Bhanage, *Mater. Lett.*, 2012, 69, 66–68.
17. C. M. Wu, J. Baltrusaitis, E. G. Gillan, V. H. Grassian, *J. Phys. Chem. C*, 2011, 115, 10164–10172.
18. <http://www.scribd.com/doc/21053651/Electronic-spectroscopy-UV-Visible>
19. Mott, N.F. and Davis, E.A., Clarendon Press, Oxford (1971).